Computer Modeling in Engineering & Sciences

Tech Science Press

DOI: 10.32604/cmes.2021.017740

ARTICLE

Fluid and Osmotic Pressure Balance and Volume Stabilization in Cells

Dedicated to Professor Karl Stark Pister for his 95th birthday

Peter M. Pinsky*

Department of Mechanical Engineering, Stanford University, Stanford, 94305, CA, USA

*Corresponding Author: Peter M. Pinsky. Email: pinsky@stanford.edu

Received: 02 June 2021 Accepted: 26 July 2021

ABSTRACT

A fundamental problem for cells with their fragile membranes is the control of their volume. The primordial solution to this problem is the active transport of ions across the cell membrane to modulate the intracellular osmotic pressure. In this work, a theoretical model of the cellular pump-leak mechanism is proposed within the general framework of linear nonequilibrium thermodynamics. The model is expressed with phenomenological equations that describe passive and active ionic transport across cell membranes, supplemented by an equation for the membrane potential that accounts for the electrogenicity of the ionic pumps. For active ionic transport, the model predicts that the intracellular fluid pressure will be balanced by the osmotic pressure and a new pressure component that arises from the active ionic fluxes. A model for the pump-leak mechanism in an idealized human cell is introduced to demonstrate the applicability of the proposed theory.

KEYWORDS

Pump-leak mechanism; cell volume regulation; active ion transport; ion pump; membrane transport; cell mechanics; modified Kedem-Katchalsky equations; nonequilibrium thermodynamics; phenomenological equations

1 Introduction

A cell must concentrate and protect within its interior substances that are essential for its function—DNA, proteins, amino acids and sugars. These sequestered substances, which are entrapped within the cell, introduce a special challenge for the cell. They carry significant concentrations of charge that establishes a high osmotic pressure within the cell. The osmotic pressure difference between the intracellular and extracellular media produces a tendency to swelling by water inflow across the cell membrane. Such swelling can be arrested by two processes: actively reducing the cellular ionic content through ion pumps, and by the generation of internal fluid pressure that can act to stop the flow of water. In fact, both processes will act simultaneously. However, animal cells have fragile membranes and it has generally been accepted that the primary action of the pump-leak mechanism (PLM) is the active reduction of cellular ionic content and the concomitant reduction in osmotic pressure. As a result, models that have been developed to explain the PLM have concentrated on osmotic stabilization due to ion pumping [1–5]. The role

of cellular fluid pressure, generated by the resistance to expansion of the cell membrane–cortex has received less attention [6–8]. A general framework for modeling the PLM including the role of fluid pressure is proposed in this work.

The movement of ions across the cell membrane occurs passively and actively. Passive transport occurs by diffusion and convection and requires no energy input. Active transport processes move ions against concentration gradients through the expenditure of energy. Both processes are important and the interplay between them, controlled by feedback [9], facilitates the regulation of cell volume, preventing potential cell rupture or collapse under changing conditions.

The cytoplasm (i.e., intracellular fluid) contains charged macromolecules and metabolites that are confined to the cell interior by entrapment and are impermeant with respect to the cell membrane—all such impermeant charged macromolecules will be referred to as fixed charges for brevity. The fixed charges localize mobile ions which form an electrical double layer of counterions and coions that screens the electric field. The resulting ion concentrations establish the osmotic pressure within the cell. If the extracellular solution has, for example, lower ionic concentrations, water will flow across the cell membrane and into the cell by osmosis, causing the cell to swell. It is the fixed charges that are essentially responsible for the swelling tendency of the cell. Active ion transporters (e.g., the Na^+ ion pump) that convert energy from various sources, including adenosine triphosphate (ATP), are located in the cell membrane and produce outward and inward fluxes of ions that modulate the osmotic and fluid pressures to arrest and reverse cellular swelling [10].

The linear theory of nonequilibrium thermodynamics has been widely employed to model passive transport processes. The approach asserts the existence of a dissipation function which describes the rate of change of entropy production. It is expressed as the sum of a set of flux and conjugate (driving) force products. For example, the classical study of Kedem et al. [11,12] used this approach to obtain the flux definitions that are conjugate to the fluid and osmotic pressures for a non-electrolyte solution. Then, considering near-equilibrium, a linear relationship between each flux and all conjugate forces is postulated. The result is a set of phenomenological equations that describes all interactions between the solvent and solutes and which is expressed with transport coefficients that have the significant merit of being amenable to experimental measurement.

When the solutes crossing the membrane are charged, the nonequilibrium thermodynamic description is more challenging and the system exhibits new features. A very general framework based on linear nonequilibrium thermodynamics has been given by Kedem et al. [13] and includes many electrokinetic phenomena within its scope. More recently, Li [14] proposed phenomenological equations for the passive transport of ionic solutions that account for electrostatic interactions between ions. This was extended by Cheng et al. [15] to account for fixed charges associated with proteoglycans for application to the corneal endothelium. The latter work identified a fluid pressure component that appears during active ion pumping and which must be considered in the balance of fluid and osmotic pressure. The goal of the present paper is to describe the temporal and steady state behavior of the pump-leak system utilizing the fully general framework of nonequilibrium thermodynamics.

We start with a brief review of the development of phenomenological equations for passive transport across a semipermeable membrane separating two ionic solutions, one of which contains impermeant charged macromolecules. Extension of the theory for active ion transport is then described, including derivation of the generalized pressure conjugate to the active ion

flux. Analytical steady state solutions are obtained for both the passive and active cases and considering an intracellular binary electrolyte solution. Solutions to the temporal problem are obtained numerically.

To illustrate the scope and features of the theory, a numerical study of a highly idealized model of a human cell is introduced. The cell is in suspension (without attachments) and is subjected to a sequence of hypotonic and hypertonic shocks. For simplicity, the intracellular and extracellular solutions are taken to be binary electrolyte solutions and the phenomenological equations are suitably specialized. The model is first applied to analyzing the response of the cell model with only passive transport. In a second analysis, active cation transport is initiated when a signal based on membrane tension is received. This simulation provides the time course of the cell radius, fluid pressure, osmotic pressures, and other quantities. The numerical results suggest that the model replicates the essential features of the PLM and that the fluid pressure component arising from the active ion flux is an essential factor in the balance of fluid and osmotic pressures, including under steady state conditions.

2 Modified Kedem-Katchalsky Equations for Passive Transport

The Kedem and Katchalsky (KK) phenomenological equations [11,12,16,17] are based on nonequilibrium thermodynamics and describe the transport of water and solutes across a semipermeable membrane separating two non-electrolyte solutions. They take the form

$$J_v = L_p \left(\Delta P - \sum_{k=1}^{N_{species}} \sigma_k RT \Delta C_k \right) \tag{1}$$

and

$$J_k = (1 - \sigma_k)\overline{C}_k J_v + \omega_k RT \Delta C_k \tag{2}$$

where J_v is the volume flow and J_k is the solute molar flux. In (1), ΔP and ΔC_k are the fluid pressure and solute concentration differences across the membrane, respectively, L_p is the hydraulic conductivity, σ_k is the reflection coefficient for species k, R is the gas constant and T is the temperature. In (2), $\overline{C}_k$ is the mean value of the solute concentration across the membrane, and ω_k is the solute permeability. These equations have found remarkably wide application in practise because the transport parameters are readily amenable to experimental measurement.

For electrolyte solutions, the transport equations should account for the electrostatic effects of the fixed and mobile ion charges. The procedure to obtain suitable modified KK phenomenological equations [14,15] is briefly reviewed as follows. The chemical potential of water with mole fraction X_w is $\mu_w = \nu_w P + RT \ln X_w$, where ν_w is the partial volume of the water and P is the fluid pressure. For dilute solutions, μ_w may be equivalently expressed in terms of the ion concentrations C_k as

$$\mu_w = \nu_w (P - RT \sum_{k=1}^{N_{species}} C_k) \tag{3}$$

where $N_{species}$ is the number of ion species. For brevity, sums over all ionic species will henceforward be indicated as $\sum$. For ionic solutes, the electrochemical potential of species k is

$$\mu_k = \nu_k P + RT \ln C_k + z_k F \psi \tag{4}$$

where v_k is the partial volume of the ion, z_k is the valence number, F is the Faraday constant and ψ is the electrostatic potential.

With reference to a biological cell, ion concentrations in the intracellular fluid are denoted C_k and in the extracellular fluid C_k^0 and membrane differences are defined to be $\Delta C_k = C_k - C_k^0$. For water $\Delta\mu_w = \mu_w^{in} - \mu_w^{out}$ and therefore, from (3),

$$\Delta\mu_w = v_w\left(\Delta P - RT\sum \Delta C_k\right) \tag{5}$$

where $\Delta P = P^{in} - P^{out}$ is the membrane fluid pressure difference. Similarly, $\Delta\mu_k = \mu_k^{in} - \mu_k^{out}$ and therefore, from (4),

$$\Delta\mu_k = v_k\Delta P + RT\ln\left(\frac{C_k}{C_k^0}\right) + z_kF\Delta\psi \tag{6}$$

where $\Delta\psi = \psi^{in} - \psi^{out}$ is the membrane potential difference. We will use the linearized form[1] of (6)

$$\Delta\mu_k = v_k\Delta P + RT\frac{\Delta C_k}{\overline{C}_k} + z_iF\Delta\psi \tag{7}$$

where $\overline{C}_k = \frac{1}{2}(C_k + C_k^0)$ is the average ionic concentration through the membrane.

The dissipation function Φ, which measures the rate of entropy production for irreversible processes, is expressed as [11,12]

$$\Phi = J_w\Delta\mu_w + \sum J_k\Delta\mu_k \tag{8}$$

where J_w and J_k are the water and ion molar fluxes, respectively, and where $\Delta\mu_w$ and $\Delta\mu_k$ are their conjugate driving forces. Instead of J_w and J_k, we seek the forces conjugate to the more readily measurable volume flow J_v and ion exchange flux J_{Dk} defined by

$$J_v = v_wJ_w + \sum v_kJ_k \tag{9}$$

and

$$J_{Dk} = \frac{J_k}{\overline{C}_k} - \frac{J_w}{C_w} \tag{10}$$

The ion exchange flux J_{Dk} may be interpreted as the velocity of ion k relative to the solvent. By direct manipulation of (8), it may be shown [15] that

$$\Phi = J_vX_v + \sum J_{Dk}X_k \tag{11}$$

[1] Since we have no knowledge of how C_k varies across the membrane, a good approximation is:

$$\ln\left(\frac{C_k}{C_k^0}\right) = \int_{C_k^0}^{C_k}\frac{dC_k}{C_k} \approx \frac{1}{\overline{C}_k}\int_{C_k^0}^{C_k} dC_k = \frac{\Delta C_k}{\overline{C}_k}$$

with $\overline{C}_k = \frac{1}{2}\left(C_k + C_k^0\right)$. For example, if $C_k = 300$ and $C_k^0 = 100$, the approximation error is 9%.

where the conjugate forces X_v and X_s are given by

$$X_v = \Delta P + RT(1 - v_w C_w) \sum \Delta C_k + \sum z_k \overline{C}_k F \Delta \psi \tag{12}$$

and

$$X_s = RT \Delta C_s + z_s \overline{C}_s F \Delta \psi - v_s \overline{C}_s \left(RT(1 - v_w C_w) \sum \Delta C_k + \sum z_k \overline{C}_k F \Delta \psi \right), \quad s = 1, 2, \ldots, N_{species} \tag{13}$$

By assuming a dilute solution such that $v_k << 1$ and $v_w C_w \approx 1$, (12) and (13) reduce to

$$X_v = \Delta P + \sum z_k \overline{C}_k F \Delta \psi \tag{14}$$

and

$$X_k = RT \Delta C_k + z_k \overline{C}_k F \Delta \psi \tag{15}$$

The flows defined in (9) and (10) are now expressed as phenomenological equations having the form

$$J_v = L_p X_v - L_p \sum \sigma_k X_k \tag{16}$$

$$J_{Ds} = -L_p \sigma_s X_v + \sum L_{Dsk} X_k, \tag{17}$$

where L_p is the hydraulic conductivity and σ_k is the reflection coefficient of species k. L_{Dsk} are permeability coefficients which satisfy the Onsager reciprocal relation such that $L_{Dsk} = L_{Dks}$, reducing the number of independent coefficients.

Under the assumption of a dilute solution we have $J_s = C_s(J_v + J_{Ds})$ which, after introducing (16) and (17), results in [15]

$$J_s = (1 - \sigma_s) \overline{C}_s J_v + \sum \omega_{sk} X_k, \quad s = 1, 2, \ldots, N_{species} \tag{18}$$

where the solute permeability coefficient $\omega_{sk} = \overline{C}_s(L_{Dsk} - L_p \sigma_s \sigma_k)$. Ignoring interactions between ions such that $\omega_{sk} = 0$ for $s \neq k$ and replacing ω_{ss} with ω_s reduces (18) to

$$J_s = (1 - \sigma_s) \overline{C}_s J_v + \omega_s X_s, \quad s = 1, 2, \ldots, N_{species} \tag{19}$$

with $\omega_s = \overline{C}_s(L_{Dss} - L_p \sigma_s^2)$ Finally, employing (14) and (15) in (16) gives the volume flux

$$J_v = L_p \left(\Delta P - \sum [\sigma_k RT \Delta C_k - (1 - \sigma_k) z_k \overline{C}_k F \Delta \psi] \right) \tag{20}$$

and likewise employing (15) in (19) gives the ion molar flux

$$J_s = (1 - \sigma_s) \overline{C}_s J_v + \omega_s (RT \Delta C_s + z_s \overline{C}_s F \Delta \psi), \quad s = 1, 2, \ldots, N_{species} \tag{21}$$

Eqs. (20) and (21) are modified forms of the KK Eqs. (1) and (2) that extends their application to electrolyte solutions by accounting for the membrane potential $\Delta \psi$. A virtue of the current formulation is that the modified equations retain the standard transport coefficients (L_p, σ_s and ω_s) that have been experimentally determined for many membranes and solutions.

An additional condition is needed to determine the membrane potential $\Delta\psi$. The assumption that the intracellular and extracellular media are electroneutral is well justified and requires

$$\sum z_k C_k + z_f C_f = 0 \tag{22}$$

and

$$\sum z_k C_k^0 = 0 \tag{23}$$

The electric current I due to passive transport of ions through channels is given by [2,5]

$$I = F\sum z_k J_k = C_{mem}\frac{d\Delta\psi}{dt} \tag{24}$$

where C_{mem} is the membrane capacitance. It is assumed that $\Delta\psi$ is changing slowly enough that the capacitive current is negligible [2], resulting in

$$\sum z_k J_k = 0 \tag{25}$$

Employing (21) in (25) and solving for $\Delta\psi$ gives

$$F\Delta\psi = -\frac{RT\sum z_k\omega_k\Delta C_k + J_v\sum z_k(1-\sigma_k)\overline{C}_k}{\sum z_k^2\omega_k\overline{C}_k} \tag{26}$$

Finally, imposing the electroneutrality conditions (22) and (23), leads to

$$F\Delta\psi = -\frac{RT\sum z_k\omega_k\Delta C_k - \left(\sum z_k\sigma_k\overline{C}_k + \frac{1}{2}z_f C_f\right)J_v}{\sum z_k^2\omega_k\overline{C}_k} \tag{27}$$

Note that this expression for $F\Delta\psi$ is implicit since J_v depends on $F\Delta\psi$. At steady state, however, $J_v = 0$ and then

$$F\Delta\psi = -\frac{RT\sum z_k\omega_k\Delta C_k}{\sum z_k^2\omega_k\overline{C}_k} \tag{28}$$

This steady state result can also be found directly from (21) when $J_s = 0$ and without recourse to the assumption on the current.

For subsequent use, the above theory is next specialized to the case of a NaCl binary electrolyte. The cation, anion and fixed charge concentrations are denoted C_1, C_2 and C_f, respectively, and have valences $z_1 = +1, z_2 = -1$ and $z_f = -1$. The extracellular solution is taken to have $C_1^0 = C_2^0 = C_0$ and contains no charged groups. For simplicity, it is assumed that the reflection coefficients and ion permeabilities are uniform for the two mobile ions so that $\sigma_1 = \sigma_2 = \sigma$ and $\omega_1 = \omega_2 = \omega$. Using the electroneutrality condition (22) to find $\sum z_k\overline{C}_k = \frac{1}{2}C_f$, the volume flux given by (20) reduces to

$$J_v = L_p\left(\Delta P - \sigma\Delta\Pi + \frac{1}{2}(1-\sigma)C_f F\Delta\psi\right) \tag{29}$$

and the ion fluxes (21) become

$$J_1 = (1-\sigma)\overline{C}_1 J_v + \omega(RT\Delta C_1 + \overline{C}_1 F\Delta\psi) \tag{30}$$

$$J_2 = (1-\sigma)\overline{C}_2 J_v + \omega(RT\Delta C_2 - \overline{C}_2 F\Delta\psi) \tag{31}$$

where the osmotic pressure $\Delta\Pi$ is

$$\Delta\Pi = RT\sum \Delta C_k = RT(C_1 + C_2 - 2C_0) \tag{32}$$

and membrane potential $\Delta\psi$ is, from (27),

$$F\Delta\psi = -\left(2RT + \frac{1-\sigma}{\omega}J_v\right)\frac{C_f}{C_1 + C_2 + 2C_0} \tag{33}$$

3 Donnan Equilibrium

Before proceeding to the case of active ion transport, we establish that the model for passive transport recovers the Donnan equilibrium pressure and concentrations. It is first established that, at equilibrium, the model predicts that $\Delta P = \Delta\Pi$ and that this holds independently of all transport coefficients. With $J_v = J_k = 0$, it follows from (21) that $\omega_k(RT\Delta C_k + z_k\overline{C}_k F\Delta\psi) = 0$, which implies

$$-(1-\sigma_k)z_k\overline{C}_k F\Delta\psi = (1-\sigma_k)RT\Delta C_k \tag{34}$$

Using this result in (20) with $J_v = 0$ gives

$$\Delta P = \sum[\sigma_k RT\Delta C_s + (1-\sigma_k)RT\Delta C_k] = \sum RT\Delta C_k = \Delta\Pi \tag{35}$$

This results confirms that $\Delta P = \Delta\Pi$ is satisfied regardless of the membrane properties, as should be the case at equilibrium.

In order to obtain the equilibrium osmotic pressure, the binary electrolyte detailed at the end of Section 2 is employed for simplicity. At equilibrium $J_v = J_1 = J_2 = 0$ and it follows from (30) and (31) that $RT\Delta C_1 + \overline{C}_1 F\Delta\psi = 0$ and $RT\Delta C_2 + \overline{C}_2 F\Delta\psi = 0$. These equations imply $\overline{C}_1\Delta C_2 + \overline{C}_2\Delta C_1 = 0$ or $C_1 C_2 = C_0^2$, which is the Donnan equilibrium condition. Using the last result with the condition of electroneutrality $C_1 - C_2 = C_f$ yields the Donnan cation and anion concentrations

$$C_1 = \frac{C_f}{2} + \sqrt{\left(\frac{C_f}{2}\right)^2 + C_0^2}; \qquad C_2 = -\frac{C_f}{2} + \sqrt{\left(\frac{C_f}{2}\right)^2 + C_0^2} \tag{36}$$

and the well-known Donnan osmotic pressure

$$\Delta\Pi = RT(C_1 + C_2 - 2C_0) = 2RTC_0\left(\sqrt{\frac{C_f^2}{4C_0^2} + 1} - 1\right) \tag{37}$$

The above results simply confirm that the passive transport model given by (20), (21) and (27) obtains the correct solution at equilibrium. We next consider the nonequilibrium problem of active ion transport.

4 Modified Kedem-Katchalsky Equations for Active Ionic Transport

Active ion transport operates to support cellular homeostasis and to prevent rupture of the cell membrane. Here we disregard the molecular-level description of ionic transport and introduce phenomenological equations for active ion transport obtained by treating the active ionic flux as an independent function of the cellular environment. It is reasonable to assume that the active ion fluxes are additive to the passive ionic flux [2,5], with the net flux expressed by

$$J_k = J_k^p + J_k^a \tag{38}$$

where J_k^p is the passive flux given by (21) and J_k^a is the active flux. The trans-membrane current due to passive and active transport of ions is then

$$I = F\sum z_k J_k = C_{mem}\frac{d\Delta\psi}{dt} \tag{39}$$

As in the passive transport case, we assume that $\Delta\psi$ is changing slowly enough that the capacitive current is negligible [2], resulting in

$$\sum z_k(J_k^p + J_k^a) = 0 \tag{40}$$

Replacing J_k^p by using (21), employing electroneutrality (22) and (23), and solving for $F\Delta\psi$ gives

$$F\Delta\psi = -\frac{RT\sum z_k\omega_k\Delta C_k - \left(\sum z_k\sigma_k\overline{C}_k + \frac{1}{2}z_f C_f\right)J_v + \sum z_k J_k^a}{\sum z_k^2\omega_k\overline{C}_k} \tag{41}$$

At steady state, $J_v = 0$ and the membrane potential is

$$F\Delta\psi = -\frac{RT\sum z_k\omega_k\Delta C_k + \sum z_k J_k^a}{\sum z_k^2\omega_k\overline{C}_k} \tag{42}$$

By comparing (41) to its value in the passive transport case (27) (or (42) to (28)), we can write

$$(F\Delta\psi)^{active} = (F\Delta\psi)^{passive} - \frac{\sum z_k J_k^a}{\sum z_k^2\omega_k\overline{C}_k} \tag{43}$$

which defines how the membrane potential changes due to active ion transport.

At steady (nonequilibrium) state, the volume flux J_v and all ion net fluxes J_k will vanish, resulting in no net transport of ions [4]. Then passive ion transport will precisely balance active ion transport for each individual species and it follows from (38) that

$$\sum z_k\overline{C}_k F\Delta\psi = -\sum\left(RT\Delta C_k + \frac{J_k^a}{\omega_k}\right) \tag{44}$$

But from (20) with $J_v = 0$ we observe that

$$\Delta P = \sum[\sigma_k RT\Delta C_s - (1-\sigma_k)z_k\overline{C}_k F\Delta\psi] \tag{45}$$

Combining the above two equations to eliminate $F\Delta\psi$ leads to the important result that the fluid pressure ΔP is given by

$$\Delta P = \Delta\Pi + \Delta P^a \tag{46}$$

where the osmotic pressure is

$$\Delta\Pi = \sum RT\Delta C_k \tag{47}$$

and where a new, additional, component of the fluid pressure pressure appears

$$\Delta P^a = \sum \frac{1-\sigma_k}{\omega_k} J_k^a \tag{48}$$

From (46) it is seen that, at steady state, the fluid pressure ΔP and osmotic pressure $\Delta\Pi$ must be balanced by the new generalized pressure term ΔP^a. This new pressure term is always present when active transport is operative, including at steady state. This term has been analyzed by numerical studies, see Section 6, which suggests that for typical ion pumping rates its magnitude is significant and comparable to the osmotic pressure.

Steady state concentrations for a binary electrolyte (as described at the end of Section 2) are found as follows. Setting $J_v = J_k = 0$ in (38) implies

$$z_k \overline{C}_k F\Delta\psi = -RT(\Delta C_k + \beta_k), \qquad k = 1,2 \tag{49}$$

where β_k (in mM units) is given by

$$\beta_k = \frac{J_k^a}{RT\omega} \tag{50}$$

Eliminating $F\Delta\psi$ from the two equations in (49) implies the Donnan-like relationship

$$\overline{C}_2(\Delta C_1 + \beta_1) + \overline{C}_1(\Delta C_2 + \beta_2) = 0 \tag{51}$$

An analogous condition has been reported in [18]. Solving this equation simultaneously with the electroneutrality condition $C_1 - C_2 = C_f$ yields the steady state concentrations

$$C_1 = \frac{1}{2}(C_f - \beta_m) + \frac{1}{2}\sqrt{(C_f - \beta_m)^2 + 4C_0(C_0 - \beta_m) + 2\beta_1 C_f} \tag{52}$$

$$C_2 = -\frac{1}{2}(C_f + \beta_m) + \frac{1}{2}\sqrt{(C_f + \beta_m)^2 + 4C_0(C_0 - \beta_m) - 2\beta_2 C_f} \tag{53}$$

where $\beta_m = \frac{1}{2}(\beta_1 + \beta_2)$. The steady state osmotic pressure $\Delta\Pi = RT(C_1 + C_2 - 2C_0)$ is then found to be

$$\Delta\Pi = 2RTC_0\left(\sqrt{\left(\frac{C_f - \beta_m}{2C_0}\right)^2 + \frac{\beta_1 C_f}{2C_0^2} - \frac{\beta_m}{C_0} + 1} - 1 - \frac{\beta_m}{2C_0}\right) \tag{54}$$

The fluid pressure contribution ΔP^a given by (48) is independent of C_1 and C_2 and may be expressed as

$$\Delta P^a = \frac{1-\sigma}{\omega}(J_1^a + J_2^a) = 2RT(1-\sigma)\beta_m \tag{55}$$

Observe that when both active ion fluxes are zero, the osmotic pressure given by (54) reduces to the Donnan equilibrium pressure (37) and ΔP^a given by (55) vanishes. These results clarify the influence of active ion fluxes at steady state on both the osmotic and fluid pressures and, as will be shown in the next section, are crucial to the osmoregulation of cell volumes.

5 A Minimal Model for Volume Osmoregulation of a Suspended Biological Cell

An application of the proposed modeling framework to cell volume osmoregulation is considered in this section, emphasizing steady state solutions for passive and active ion transport. The transient solution for osmotic shock loading is developed in Section 6. We consider a suspended biological cell that has spherical geometry. The cell cytoplasm and extracellular fluid are taken to be the binary electrolyte described at the end of Section 2. The cell will undergo volume expansion and contraction according to osmotic conditions.

Assuming that the number of lipid molecules in the membrane is conserved, it may be shown that the stretching free energy dominates the curvature free energy and the structural behavior of the cell cortex—lipid membrane system can therefore be modeled to first order as an elastic shell with area elasticity. The spherical elastic shell has a tension-free reference area A_0 and radius r_0 and current radius $r(t)$ and area $A(t)$. The membrane tension τ in N/m is assumed to be related to the cell surface area by

$$\tau = K\left(\frac{A-A_0}{A_0}\right) = K\left(\frac{r^2-r_0^2}{r_0^2}\right) \tag{56}$$

where K is the area elasticity constant. Using elementary statics, equilibrium requires $\tau = \frac{1}{2}r\Delta P$, where ΔP is the fluid pressure difference across the membrane, leading to

$$\Delta P = \frac{2K}{r}\left[\left(\frac{r}{r_0}\right)^2 - 1\right] \quad \text{or} \quad r = \frac{\Delta P r_0^2}{4K} + \sqrt{\left(\frac{\Delta P r_0^2}{4K}\right)^2 + r_0^2} \tag{57}$$

Using $(57)_1$ in the expression for the volume flux J_v given by (29) and noting that $\Delta\Pi = RT(C_1 + C_2 - 2C_0)$ results in

$$J_v = L_p\left(\frac{2K}{r}\left[\left(\frac{r}{r_0}\right)^2 - 1\right] - \sigma RT(C_1 + C_2 - 2C_0) + \frac{1}{2}(1-\sigma)C_f F\Delta\psi\right) \tag{58}$$

The cell radius $r(t)$, in m, and volume flux J_v, in $m^3/m^2 - s$, can be related by observing that the rate of volume expansion of the spherical cell is $4\pi r^2\frac{dr}{dt}$ in m^3/s. This expansion rate must be

balanced by a fluid volume influx of $-4\pi r^2 J_v$, where J_v is given by (58); the negative sign appears because positive J_v is defined as a flow from the cell to the extracellular fluid. Then,

$$\frac{dr}{dt} + J_v = 0 \tag{59}$$

We next establish a relation between the ion concentrations and the cell radius. The total number of moles of ion species k occupying the cell is $n_k = \frac{4}{3}\pi r^3 C_k$. Then the rate of change $\frac{dn_k}{dt} = \frac{4}{3}\pi r^3 \frac{dC_k}{dt} + 4\pi r^2 \frac{dr}{dt} C_k$ must be balanced by a net surface influx of ions $-4\pi\, r^2 J_k$, where J_k is the net molar flux in $mol/m^2 - s$ and where the negative sign again derives from the definition of J_k. The conservation of ions then requires

$$\frac{r}{3}\frac{dC_k}{dt} + \frac{dr}{dt} C_k + J_k = 0, \qquad k = 1, 2 \tag{60}$$

which describes an evolution equation for the concentration C_k. The molar flux J_k has the additive form given by (38). Specializing the passive component J_k^p for the binary electrolyte (see (30) and (31)) and using (59) to replace J_v, gives

$$J_k = -(1-\sigma)\overline{C}_k \frac{dr}{dt} + \omega(RT\Delta C_k + z_k \overline{C}_k F \Delta\psi) + J_k^a, \qquad k = 1, 2 \tag{61}$$

The membrane potential is given by (41) which, for the binary electrolyte and again using (59) to replace J_v, reduces to

$$F\Delta\psi = \left[\left(\frac{1-\sigma}{\omega}\frac{dr}{dt} - 2RT\right) C_f - \frac{2}{\omega}(J_1^a - J_2^a)\right] \frac{1}{C_1 + C_2 + 2C_0} \tag{62}$$

The cell model framework is given by the three coupled ODEs (59) and (60), with the volume flux J_v and ion fluxes J_k given by (58) and (61), respectively, and the membrane potential by (62). This system can be solved numerically for $r(t), C_1(t)$ and $C_2(t)$ after specification of the functions J_1^a and J_2^a and suitable initial conditions on r, C_1 and C_2. The coupled system (59) and (60) is nonlinear only in variable r. The transient transport model is discussed in Section 6; the focus in this section is on steady state solutions for passive and active ion transport.

Starting with passive transport ($J_1^a = J_2^a = 0$) at steady state $\left(\frac{dr}{dt} = \frac{dC_1}{dt} = \frac{dC_2}{dt} = 0 \text{ and } J_v = J_1 = J_2 = 0\right)$, the Donnan equilibrium osmotic pressure $\Delta\Pi$ is given by (37). Noting that $\Delta P = \Delta\Pi$ at equilibrium and substituting (37) into $(57)_2$ gives the equilibrium cell radius

$$r = \frac{RTC_0 r_0^2}{2K}\left(\sqrt{\frac{C_f^2}{4C_0^2} + 1} - 1\right) + \sqrt{\left(\frac{RTC_0 r_0^2}{2K}\right)^2 \left(\sqrt{\frac{C_f^2}{4C_0^2} + 1} - 1\right)^2 + r_0^2} \tag{63}$$

Fig. 1 depicts the equilibrium radius r computed for parameter values that are representative for human cells (see Table 1) and for variations in the fixed charge concentration C_f and extracellular ion concentration C_0. Fig. 1 shows that both have an important influence on the cell

equilibrium radius. The equilibrium radius r is independent of all membrane transport properties and provides a reference value for examining the effect of active ion transport, which is considered next.

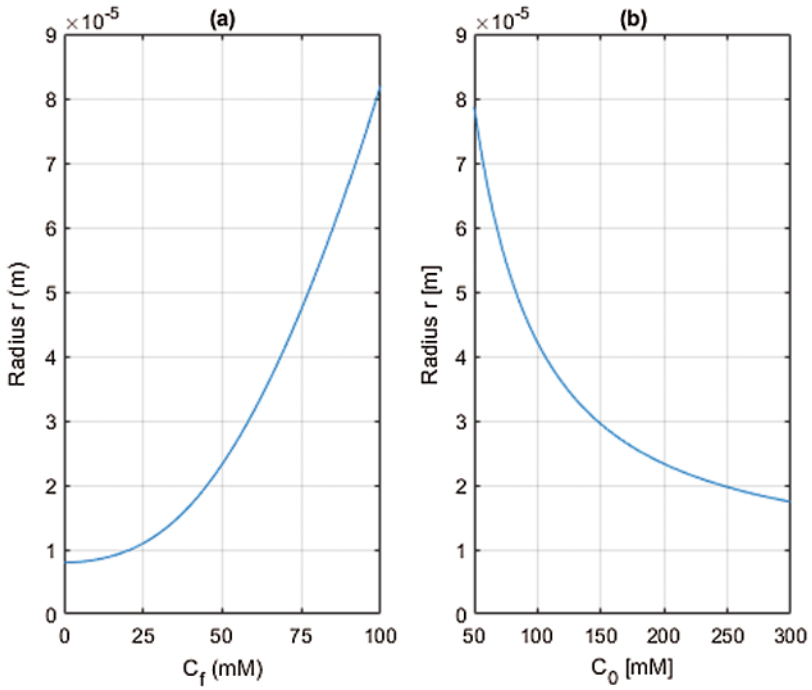

Figure 1: Steady state cell radius r computed from Eq. (63) with $r_0 = 8 \times 10^{-6}\ m$ and $K = 1.25 \times 10^{-2}\ N/m$. (a) Variation of fixed charge concentration C_f with extracellular concentration $C_0 = 200\ mM$, (b) Variation of extracellular concentration C_0 with fixed charge concentration $C_f = 50\ mM$

Table 1: Physical constants and model parameters used in simulations and representative of a human cell

Parameter	Description	Units	Value
r_0	Reference (unloaded) cell radius	m	8×10^{-6}
K	Membrane area elasticity	N/m	1.25×10^{-2}
C_0	Extracellular fluid concentration	mM	200
T	Temperature	K	310
R	Gas constant	$N-m/mol-K$	8.3144598
C_f	Fixed charge concentration in cell	mM	50
σ	Reflection coefficient	1	0.5
L_p	Hydraulic conductivity	$m/Pa-s$	1×10^{-10}
ω	Solute permeability	$mol/N-s$	1×10^{-9}

For active ion transport at steady (nonequilibrium) state $\left(\frac{dr}{dt}=\frac{dC_1}{dt}=\frac{dC_2}{dt}=J_v=J_1=J_2=0\right.$ with $J_1^a\neq 0$ and/or $J_2^a\neq 0$ and steady), the fluid pressure is given by $\Delta P=\Delta\Pi+\Delta \mathrm{P}^a$ (see (46)). The steady state cell radius for active ion transport is then found from $(57)_2$ as

$$r=\frac{r_0^2}{4K}(\Delta\Pi+\Delta P^a)+\sqrt{r_0^2+\left(\frac{r_0^2}{4K}\right)^2(\Delta\Pi+\Delta P^a)^2} \tag{64}$$

where $\Delta\Pi$ and $\Delta \mathrm{P}^a$ are evaluated using (54) and (55), respectively.

Fig. 2 examines the steady state cell radius based on (64) resulting from active transport of the cation only with $\beta_1=J_1^a/(RT\omega)$ and $\beta_2=0$. All parameters employed are taken from Table 1. The steady state cell radius depicted in Fig. 2 demonstrates the steady state limit of the pump-leak mechanism in which active ion pumping reduces the osmotic pressure, causing the cell volume to contract as water passively transports out across the cell membrane. The effect of cation pumping on the steady state fluid and osmotic pressures are examined next.

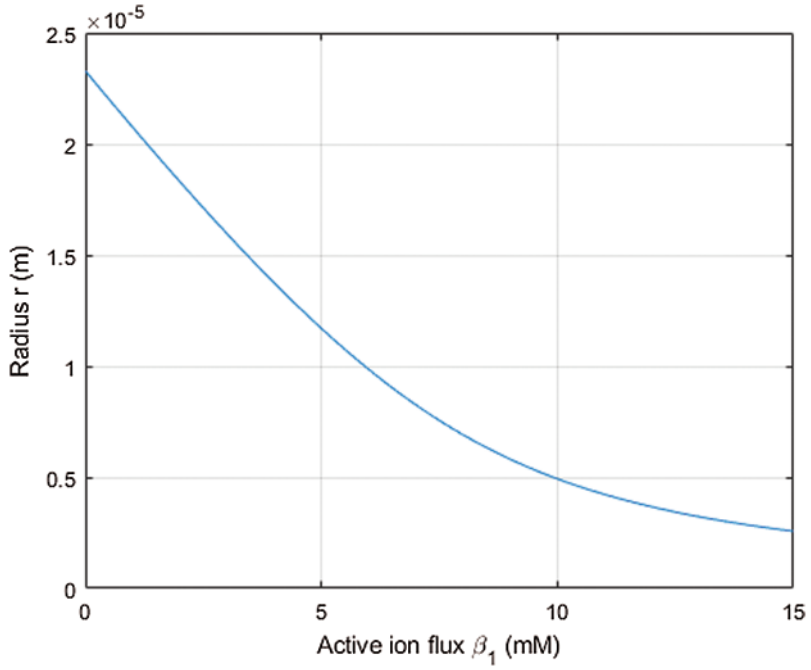

Figure 2: Steady state cell radius r (m) with active cation transport as measured by β_1 (mM) and with $\beta_2=0$. The cell properties are taken from Table 1. Increasing the cation pumping rate β_1 decreases the steady state cell radius

The steady state values of $\Delta\Pi$ and ΔP^a are plotted in Fig. 3 against β_1 using (54) and (55), along with ΔP derived from $\Delta P=\Delta\Pi+\Delta \mathrm{P}^a$. As active cation transport increases through β_1, both osmotic and fluid pressure decrease significantly. The difference between them is $\Delta \mathrm{P}^a$, which increases with β_1. Thus the fluid pressure reduction trails that of the osmotic pressure. It can be observed from Fig. 3 that at $\beta_1\approx 7\,mM$, the fluid pressure difference becomes negative and the membrane state will transition from tension to compression. This is confirmed by Fig. 2 which

indicates that the steady state equilibrium radius at $\beta_1 = 7\,mM$ is $r = 8 \times 10^{-6}\ m$, which is the cell reference radius r_0. Fig. 3 demonstrates quantitatively how increasing active ion transport reduces the osmotic and fluid pressures and thereby provides cell volume osmoregulation. The temporal solution of the model system (59) and (60) provides further insights into the PLM and is considered next.

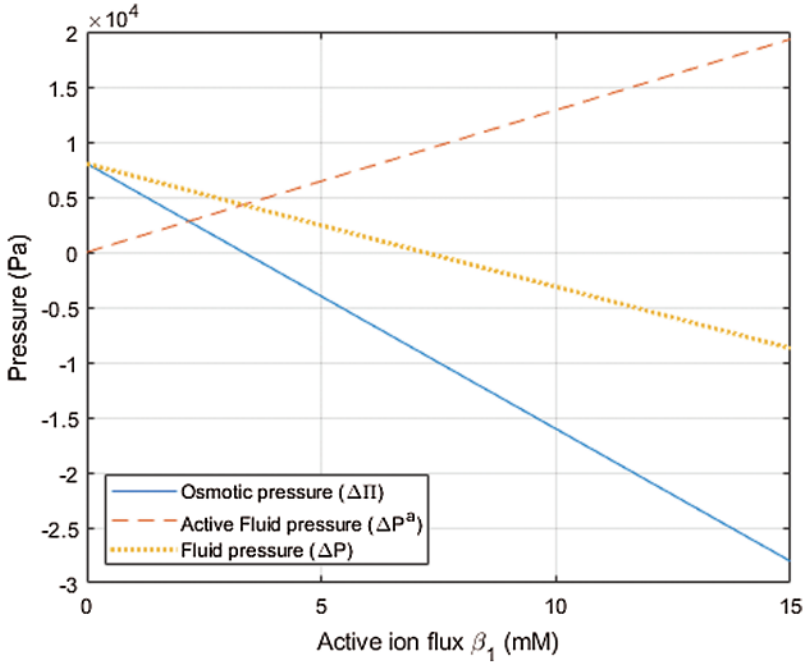

Figure 3: Plot of osmotic pressure $\Delta\Pi$, active fluid pressure ΔP^a and fluid pressure ΔP *vs.* active cation flux β_1 (with no anion active flux $\beta_2 = 0$). Cell properties are taken from Table 1

6 Temporal Response of the Pump-Leak Mechanism

6.1 Cell Response Simulations

Characterizing the details of ion channels and pumps is an active area of research that is beyond the scope of the present work. Nevertheless, a primitive example of an ion channel control model for homeostasis is provided in Section 6.3 to illustrate the ability of the proposed phenomenological equations to describe the pump-leak mechanism (PLM).

Two sets of numerical simulations are presented. In the first, the temporal response of the cell with only passive ion transport to a sequence of osmotic shocks is described in Section 6.2. Steady state results inferred from the temporal analysis are compared to the theoretical predictions given in Section 5 and provide a consistency check for the numerical implementation. In the second set of calculations, the PLM is simulated with active cation pumping. The initiation of active cation (Na^+) pumping occurs when a tension-based cell membrane signal is received and subsequent changes in cell volume, fluid and osmotic pressure are reported in Section 6.3.

The physical constants and model parameter values given in Table 1 are used in all simulations, unless otherwise noted.

6.2 *Passive Ionic Transport with Osmotic Shock*

The cell was given arbitrary initial values of $r(0) = 8 \times 10^{-6}\ m$, $C_1(0) = 210\ mM$ and $C_2 = 190\ mM$, and allowed $1000\ s$ to achieve near steady state. The cell is then subject to a hypotonic shock at $t = 1000\ s$ in which the extracellular ionic concentration C_0 reduces from 200 to 120 mM. This is followed by a hypertonic shock at $t = 2000\ s$ in which C_0 increases from 120 to 480 mM. This is described by

$$C_0(t) = 200[1 - 0.4H(t - 1000) + 1.8H(t - 2000)] \tag{65}$$

where H is the Heaviside step function[2]. Solution of the three coupled ODEs (59) and (60), with $\beta_1 = \beta_2 = 0$ (no active ion pumping), was obtained using commercial software *COMSOL Multiphysics 5.5*. As seen in Fig. 4, the time interval between the initial (arbitrary) state and application of the two shocks was sufficient to allow the solution to closely approach three equilibrium states. As a validation of the temporal solution, the steady state radius and (Donnan) ionic concentrations and osmotic pressure was computed using (63), (36) and (37), respectively, at the three step levels of C_0 in (65) and are given in Table 2. It may be confirmed from Fig. 4 that these values are the steady state asymptotes achieved in the temporal solution.

Table 2: Steady state (equilibrium) solutions at three levels of the extracellular ionic concentration C_0

C_0	mM	200	120	480
r	$1 \times 10^{-6}\ m$	23.3	35.8	13.4
C_1	mM	226.6	147.6	505.7
C_2	mM	176.6	97.6	455.7
$\Delta\Pi$	KPa	8.0	13.3	3.4

It may be observed in Fig. 4 that the cell radius achieves equilibrium at a slower rate than the ionic concentrations. This is expected because the rate of water transport across the membrane is controlled by the hydraulic conductivity L_p. When the hypotonic shock is applied at $T = 1000\ s$, the volume flux J_v shown in Fig. 4d jumps to a negative value, indicating water inflow, but the slow tail of the passive inflow accounts for the slow response of the cell volume. Similarly, when the hypertonic shock is applied, the volume flux jumps to a positive value, indicating water outflow, with a time course dictated by the constant hydraulic conductivity. It may be noted from Fig. 4c that the osmotic pressure in the cell increases after the hypotonic shock and reduces after the hypertonic shock, as expected. Fig. 4b indicates that the cation and anion concentrations satisfy electroneutrality $C_1 - C_2 = C_f = 50\ mM$ at all times. It is remarked that the cell generates fluid pressure (not shown) by virtue of the elastic cortex—lipid membrane system and at steady state it is indeed in Donnan equilibrium.

[2] The Heaviside functions $H(t - t_{shock})$ were smoothed over a transition zone of $100\ s$ in order to be more physically realistic.

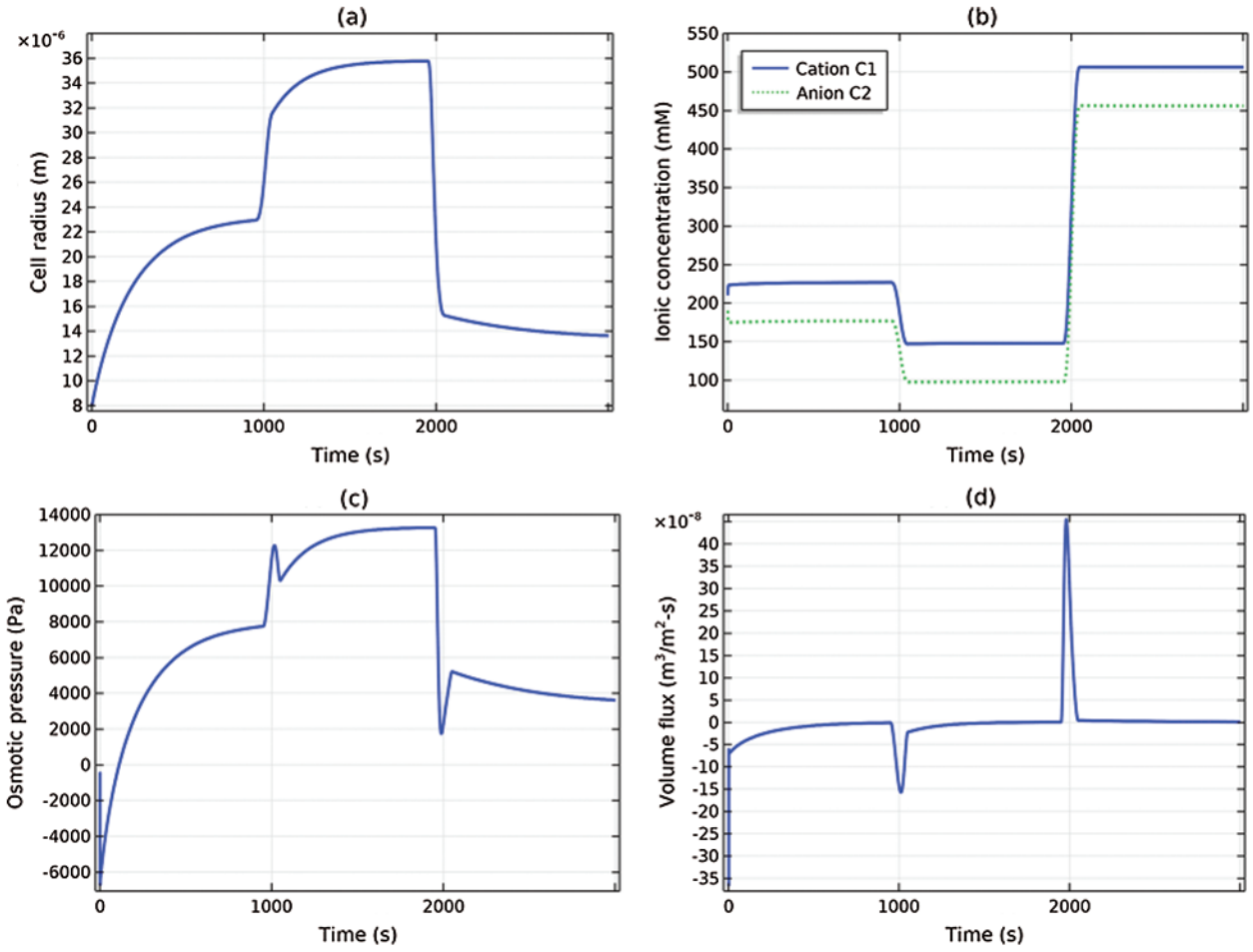

Figure 4: Transient response of the cell, with only passive ionic transport, to the osmotic shock loading given by (65): (a) Cell radius, (b) cation and anion concentrations, (c) osmotic pressure, (d) volume flux

6.3 Active Ionic Transport with Osmotic Shock

Using the same arbitrary initial values noted in the preceding subsection, 1000 s is allowed for the system to reach near steady state. The cell is then subject to a single hypotonic shock at $t = 1000\ s$ according to

$$C_0(t) = 200[1 - 0.6H(t - 1000)] \tag{66}$$

Active cation (Na^+) pumping is initiated when the membrane tension $\tau = \tau_{crit}$. For this simulation, we assumed $\tau_{crit} = 5 \times \tau_{physio}$ where τ_{physio} is the membrane tension when the cell is at equilibrium with $C_0 = 200\,mM$. Cation pumping is described by the value of β_1 (see (50)), which was taken to be constant once activated. Then active transport by cation pumping is described by

$$\beta_1(t) = \overline{\beta}_1 H(\tau(t) - \tau_{crit}) \quad \text{and} \quad \beta_2(t) = 0 \tag{67}$$

with active flux magnitude $\overline{\beta}_1 = 8.54\ mM$.

Fig. 5 compares two solutions. The solid (blue) curves correspond to passive transport only $\beta_1(t) = \beta_2(t) = 0$) and the dotted (green) curves correspond to the active transport case defined by (67). It is remarked that the active flux magnitude $\overline{\beta}_1$ was selected to approximately return the cell radius to its previous steady state value—a parametric study on β_1 is provided below. Fig. 5 indicates that cation pumping was initiated, according to (67), at approximately $t = 1{,}250\ s$ and that it has a pronounced effect on all solution variables. Most notably, the cell swells (measured by the radius r) under passive transport conditions following application of the shock. It then deswells under active transport conditions. The activation of cation pumping changes the cation molar flux from inflow to outflow Fig. 5b, and significantly depresses the osmotic pressure Fig. 5c. It may be confirmed that the steady state radius for the passive and active cases shown in Fig. 5 are predicted by (63) and (64), respectively.

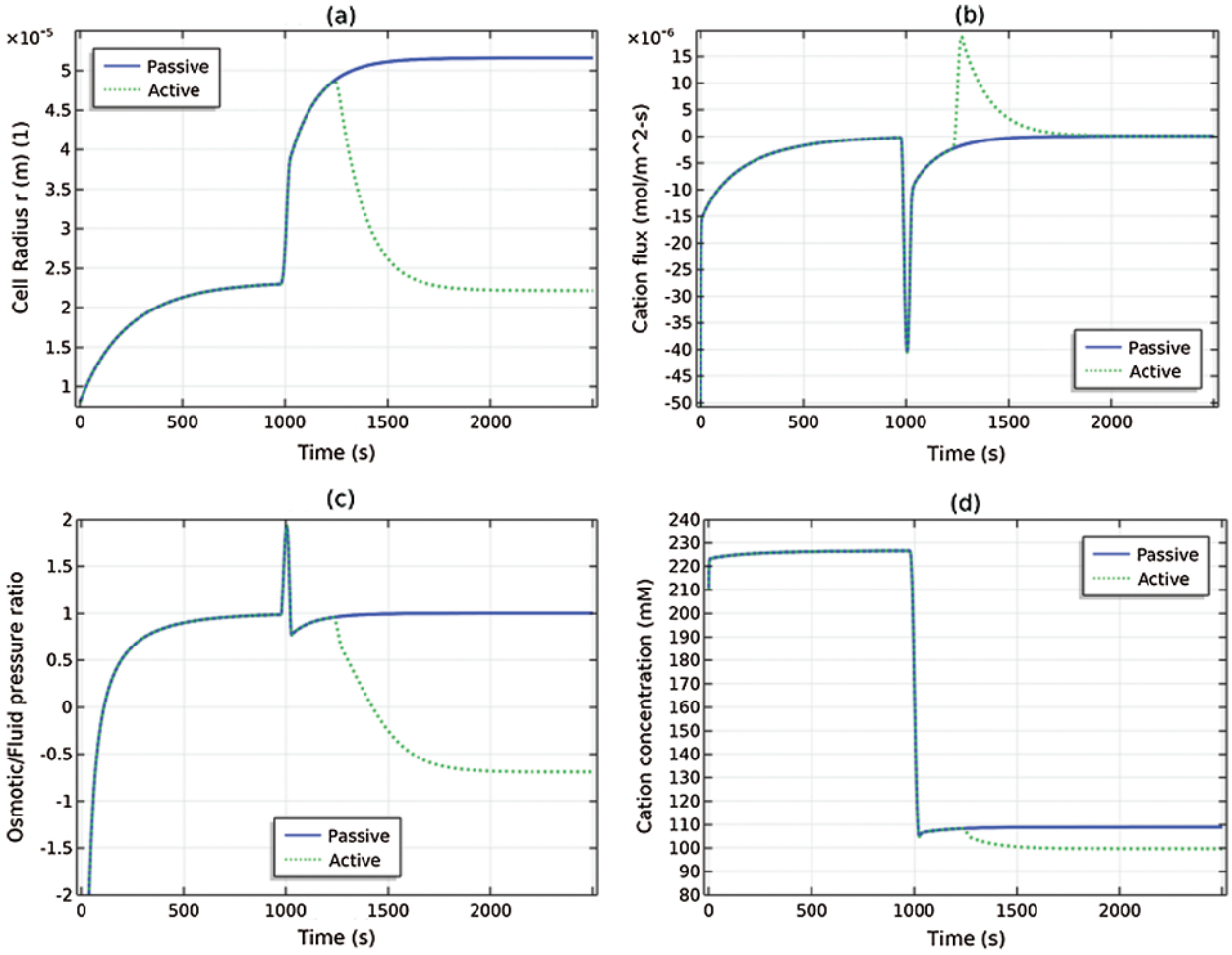

Figure 5: The cell is subjected to a hypotonic shock at $t = 1000\ s$ and two solutions are depicted. The solid (blue) curve shows the passive transport case and the dotted (green) curves show the active transport case: (a) cell radius $r(t)$, (b) cation flux $J_1(t)$, (c) ratio of osmotic and fluid pressure $\Delta P(t)/\Delta\Pi(t)$, and (d) cation concentration $C_1(t)$

Fig. 6a shows a side-by-side comparison of the osmotic and fluid pressures for the passive transport solution; Fig. 6b shows the same comparison for the active transport solution. It is seen from Fig. 6a that at steady (equilibrium) state ($t = 1000$ and $t = 3000$ s), the fluid and osmotic pressures coincide (as necessary, see (35)), whereas in Fig. 6b the osmotic and fluid pressures deviate significantly at steady (nonequilibrium) state ($t = 3000$ s) due to the active cation transport. The difference between the osmotic and fluid pressures is the active pressure component $\Delta \mathrm{P}^a = \Delta P - \Delta \Pi$ given by (48). At steady state ($t = 3000$ s) and using (55), $\Delta P^a = 2RT(1-\sigma)\beta_m \approx 11$ kPa; from Fig. 6b we see that $\Delta P \approx 6$ kPa and $\Delta \pi \approx -5$ kPa, which is in agreement. Observe that ΔP^a is of the same order as ΔP and $\Delta \Pi$ for ion pumping at $\overline{\beta}_1 = 8.54$ mM.

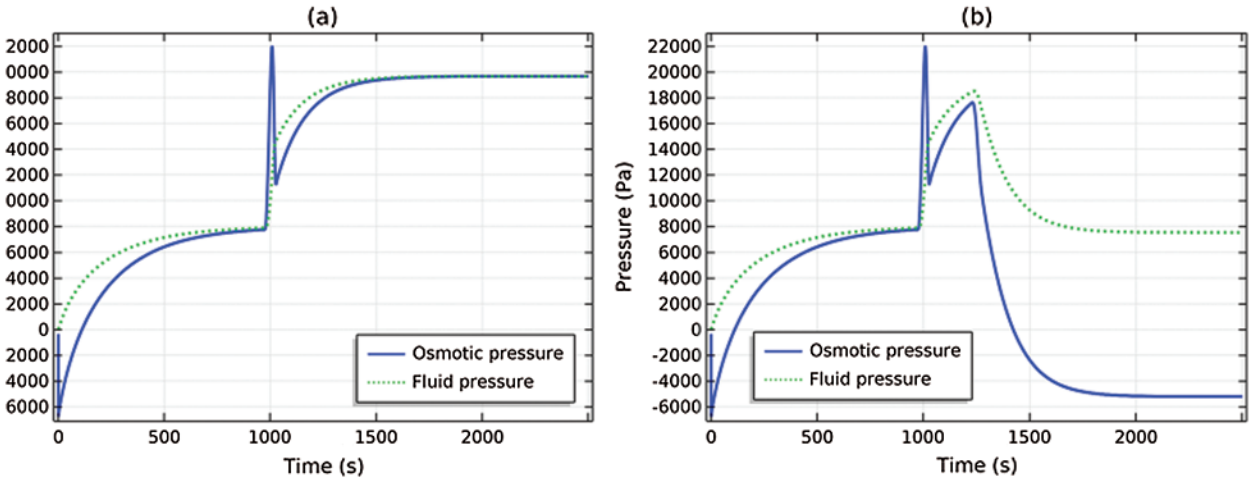

Figure 6: Comparison of osmotic and fluid pressures. (a) Passive transport solution, (b) Active cation transport solution

The results of a parametric study of the osmotic shock problem (67) is provided in Fig. 7. Figs. 7a and 7b show the cell radius and osmotic pressure for $\beta_1 = \{3, 6, 9\}$; the radius and osmotic pressure decrease with increasing cation pump rate β_1. Figs. 7c and 7d show the cell radius and osmotic pressure for the reflection coefficient $\sigma = \{1, 0.5, 0\}$ and β_1 given by (67). When $\sigma = 1$, the membrane is semipermeable and the cation cannot transport passively across the membrane. At this limiting value of σ and at steady state, we have $\Delta P^a = 0$ (see (55)) and the fluid and osmotic pressures will agree. When $\sigma = 0.5$ (the reference state used in Table 1), the membrane is leaky and the cation is transported passively and actively. When $\sigma = 0$, the membrane is nonselective and the cation is freely transported.

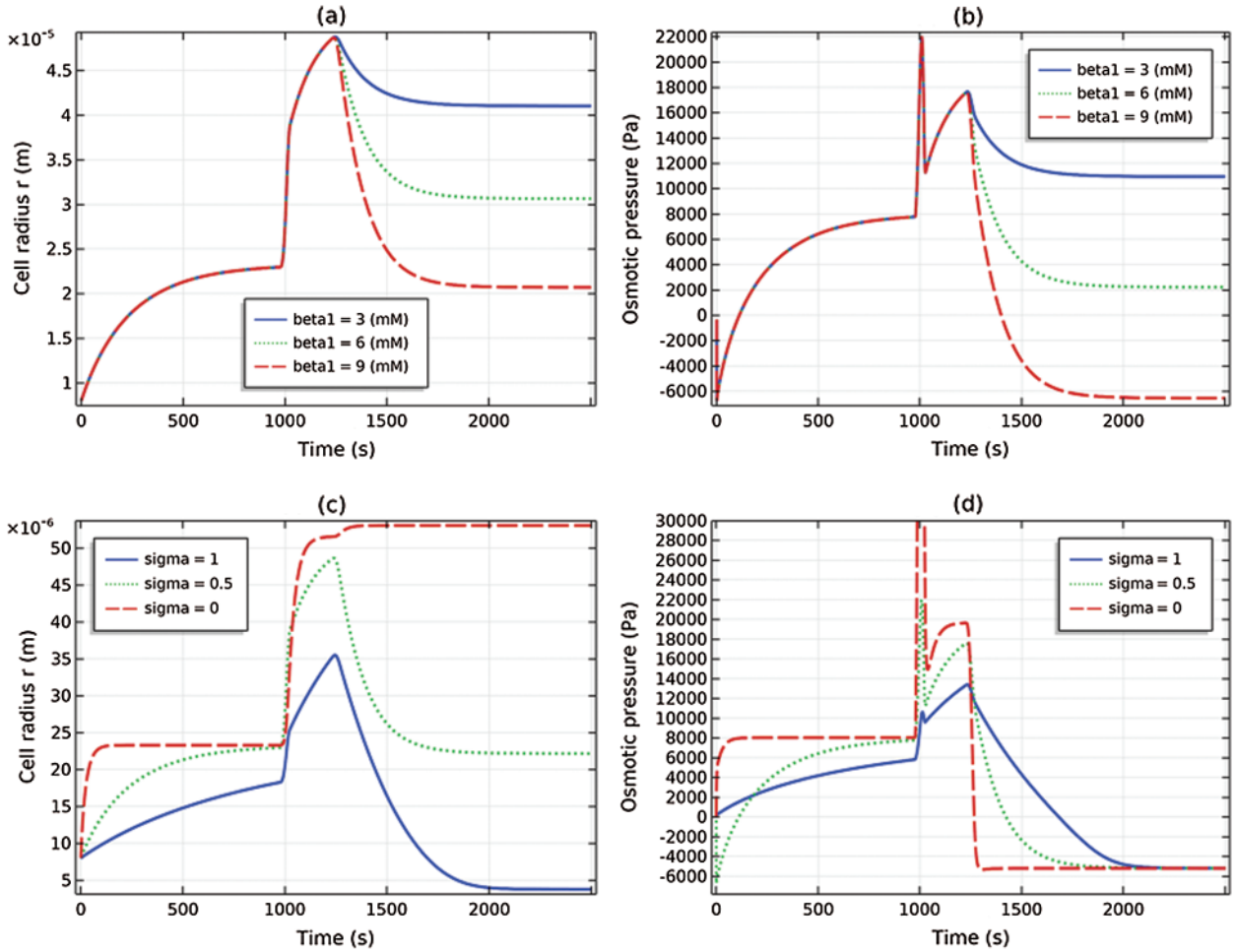

Figure 7: Parametric studies. (a) and (b) Active cation flux magnitude $\beta_1 \in [3, 6, 9]\ mM$, (c) and (d) reflection coefficient $\sigma \in [1, 0.5, 0]$

7 Discussion

The presented development of the phenomenological equations for passive and active transport for cell membranes follows standard lines for nonequilibrium thermodynamics. But an important step for electrolytes with impermeant charged macromolecules included the incorporation of fixed charge through the condition of electroneutrality. For passive transport of ionic solutions and at steady state, the theory recovers the Donnan equilibrium and predicts agreement of the osmotic and fluid pressure differences across the membrane such that $\Delta P = \Delta\Pi$. When active ion transport processes are present, the theory predicts that an active fluid pressure component ΔP^a arises as a direct result of the active fluxes. This term enters into the balance of fluid and osmotic pressure such that $\Delta P = \Delta\Pi + \Delta P^a$. When the membrane is leaky, with $\sigma < 1$, numerical results indicate that ΔP^a can have values that are of the same order as $\Delta\pi$. The presented theory has included the fluid pressure in a rigorous manner through the phenomenological equations providing a general framework for assessing its role in the PLM.

The model evaluated the membrane potential $\Delta\psi$ by using the assumption that it is not changing rapidly with time. This led to the condition that the sum of the active and passive

currents vanish $I^p + I^a = 0$. The resulting expressions for $\Delta\psi$ (see (41)) generalize previous models such as that presented by Armstrong [2] to include the influence of the ionic reflection coefficient σ_k and ionic permeability ω_k.

Following presentation of the general theory for an arbitrary number of ionic species, the theory was adapted to model the pump-leak mechanism (PLM) in a eukaryotic cell model. The cell was modeled as a spherical elastic shell with area elasticity but no attempt was made to model the dependence of the modulus on the cell volume or other possible structural characteristics. However, the cell cortex—lipid membrane system so modeled was able to develop tension and support fluid pressure—allowing both fluid and osmotic pressures to be modeled and studied for both passive and active transport. The intracellular and extracellular media were taken to be simple binary electrolytes containing Na^+ and Cl^- ions. Trapped (nonpermeant) charged macromolecules were included in the intracellular medium but no attempt was made to model the "excluded volume" effects associated with the molecular volumes (this is essentially treated by specification of an effective charge concentration C_f). Temporal changes in concentrations took account of membrane transport processes and the dynamically evolving cell area and volume. Active ion transport results were reported using an Na^+ pump to stabilize cell volume against osmotic forces that would otherwise drive water into the cell.

The PLM mechanism is clearly demonstrated in Fig. 8. The problem solved is that described in Section 6.3; the cell is subjected to a hypotonic shock at time $t = 1000\ s$, at which time it begins to swell as indicated by the increasing cell radius and the jump in water inflow (negative values of J_v). Initiation of Na^+ pumping occurs when the membrane tension reaches a critical value, at time $t \approx 1{,}250\ s$. The cell volume now starts to decrease and approach a steady state. The direct correlation of Na^+ active flux with water outflow (positive values of J_v) is apparent in the figure and suggests capture of the PLM.

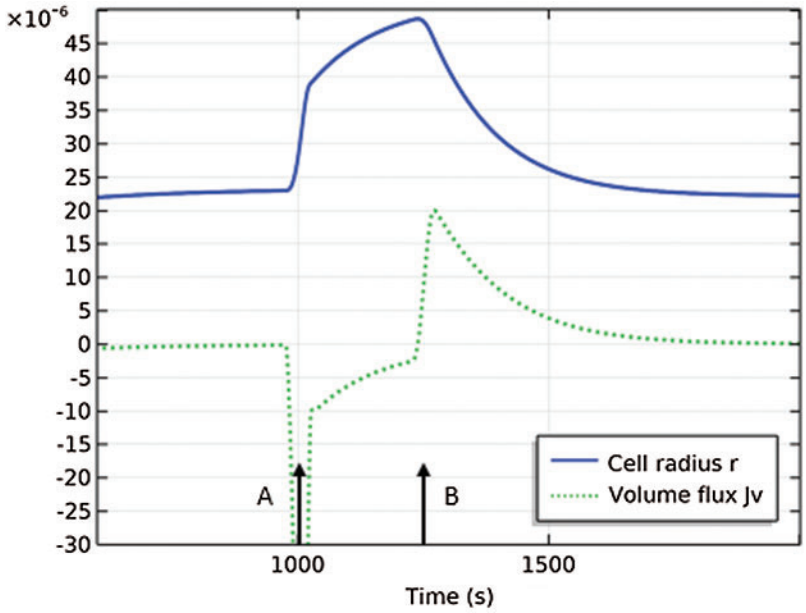

Figure 8: Cell undergoes hypotonic shock at time A and initiates active cation pumping at time B. The cell radius is $r(m)$ and the volume flux is J_v $(mol/m^2 - s)$ and has been scaled by 120. At time A, the cell begins to swell by water inflow. At time B, the cell begins to deswell by water outflow

Previous models of the PLM, presented in the field of mathematical physiology have been successful in demonstrating the key aspects of the mechanism [2,3,5,19]. However these models cannot exhibit a stable Donnan equilibrium, in contrast to the current study. Cells cannot be at a stable Donnan equilibrium unless they can develop and sustain a transmembrane fluid pressure. For example, in prior models, if ions are not actively pumped, the cell volume will increase without limit and no steady state will be found. The current model develops fluid pressure and arrives at steady state according to the hydraulic conductivity (see, for example, Fig. 5a). It has been claimed that cells cannot be at a stable Donnan equilibrium, but this is true only if they cannot support internal fluid pressure [20]. The current model shows clearly that in the case of passive ion transport, Donnan equilibrium can be achieved using realistic values of the cell membrane elasticity.

In practice, the primary contributors to intracellular and extracellular tonicity are Na^+, K^+ and Cl^- , all of which are permeable solutes. The Na^+ pump (Na^+- K^+ ATPase) actively drives Na^+ out and K^+ in [5,21]. Ion channels and ion pumps drive the physiological system, aquaporins (water channels) likewise modulate the hydraulic conductivity of the cell membrane. These essential features underlying the PLM can be modeled within the presented framework, based on experimental evidence, and would provide a more complete representation of the PLM.

Funding Statement: The author received no specific funding for this study.

Conflicts of Interest: The author declares that they have no conflicts of interest to report regarding the present study.

References

1. Hoffmann, E., Lambert, I., Pedersen, S. (2009). Physiology of cell volume regulation in vertebrates. *Physiological Reviews, 89(1),* 193–277. DOI 10.1152/physrev.00037.2007.
2. Armstrong, C. (2003). The Na/K pump, Cl ion, and osmotic stabilization of cells. *Proceedings of the National Academy of Sciences, 100(10),* 6257–6262. DOI 10.1073/pnas.0931278100.
3. Kay, A. (2017). How cells can control their size by pumping ions. *Frontiers in Cell and Developmental Biology, 5(41),* 1–14. DOI 10.3389/fcell.2017.00041.
4. Kay, A., Blaustein, M. (2009). Evolution of our understanding of cell volume regulation by the pump-leak mechanism. *Journal of General Physiology, 151(4),* 407–416. DOI 10.1085/jgp.201812274.
5. Keener, J., Sneyd, J. (2009). *Mathematical physiology I: Cellular physiology*. Second edition. New York: Springer.
6. Stewart, M., Helenius, J., Toyoda, Y., Ramanathan, S., Muller, D. et al. (2011). Hydrostatic pressure and the actomyosin cortex drive mitotic cell rounding. *Nature, 469,* 226–230. DOI 10.1038/nature09642.
7. Jiang, H., Sun, S. (2013). Cellular pressure and volume regulation and implications for cell mechanics. *Biophysical Journal, 105(3),* 609–619. DOI 10.1016/j.bpj.2013.06.021.
8. Charras, G., Yarrow, J., Horton, M., Mahadevan, L., Mitchison, T. (2005). Non-equilibration of hydrostatic pressure in blebbing cells. *Nature, 435,* 365–369. DOI 10.1038/nature03550.
9. Fraser, J., Middlebrook, C., Usher-Smith, J., Schwiening, C., Huang, C. (2005). The effect of intracellular acidification on the relationship between cell volume and membrane potential in amphibian skeletal muscle. *The Journal of Physiology, 563,* 745–764. DOI 10.1113/jphysiol.2004.079657.
10. Dawson, D., Liu, X. (2009). Osmoregulation: Some principles of water and solute transport. In: D. Evans (ed.), *Osmotic and ionic regulation: Cells and animals*. pp. 1–35. Boca Raton, FL: CRC Press.
11. Kedem, O., Katchalsky, A. (1958). Thermodynamic analysis of the permeability of biological membranes to non-electrolytes. *Biochimica et Biophysica Acta, 27(2),* 229–246. DOI 10.1016/0006-3002(58)90330-5.
12. Friedman, M. (2008). *Principles and models of biological transport*. Second edition. New York: Springer.

13. Kedem, O., Katchalsky, A. (1963). Permeability of composite membranes. Part 1. Electric current, volume flow and flow of solute through membranes. *Transactions of the Faraday Society, 59,* 1918–1930. DOI 10.1039/TF9635901918.
14. Li, L. (2004). Transport of multicomponent ionic solutions in membrane systems. *Philosophical Magazine Letters, 84(9),* 593–599. DOI 10.1080/09500830512331325767.
15. Cheng, X., Pinsky, P. (2015). The balance of fluid and osmotic pressure across active biological membranes with application to the corneal endothelium. *PLoS One, 10(12)*. DOI 10.1371/journal.pone.0145422.
16. Demirel, Y., Sandler, S. (2002). Thermodynamics and bioenergetics. *Biophysical Chemistry, 97(2),* 87–111. DOI 10.1016/S0301-4622(02)00069-8.
17. Schultz, S. (1980). *Basic principles of membrane transport,* New York: Cambridge University Press.
18. Adar, R., Safran, S. (2020). Active volume regulation in adhered cells. *Proceedings of the National Academy of Sciences, 117(11),* 5604–5609.
19. Mori, Y. (2012). Mathematical properties of pump-leak models of cell volume control and electrolyte balance. *Journal of Mathematical Biology, 65,* 875–918. DOI 10.1007/s00285-011-0483-8.
20. Sperelakis, N., (2012). Gibbs-donnan equilibrium potentials. In: N. Sperelakis (Ed.), *Cell physiology sourcebook*. Third edition, pp. 147–151. New York: Academic Press.
21. Stein, W. (1995). The sodium pump in the evolution of animal cells. *Philosophical Transactions of the Royal Society of London. Series B: Biological Sciences, 349,* 263–269. DOI 10.1098/rstb.1995.0112.